Reworking subducted sediments in arc magmas and the isotopic diversity of the continental crust: The case of the Ordovician Famatinian crustal section, Argentina

J Cornet, Oscar Laurent, J-F Wotzlaw, M A Antonelli, J Otamendi, G W Bergantz, O Bachmann

Earth and Planetary Science Letters 595 (2022) 117706

Contents lists available at ScienceDirect

Earth and Planetary Science Letters

www.elsevier.com/locate/epsl

Reworking subducted sediments in arc magmas and the isotopic diversity of the continental crust: The case of the Ordovician Famatinian crustal section, Argentina

J. Cornet [a,*], O. Laurent [a,b], J.-F. Wotzlaw [a], M.A. Antonelli [a], J. Otamendi [c], G.W. Bergantz [d], O. Bachmann [a]

[a] ETH Zürich, Department of Earth Sciences, Institute for Geochemistry and Petrology, Zürich, Switzerland
[b] CNRS, Observatoire Midi-Pyrénées, Géosciences Environnement Toulouse, 14 avenue E. Belin, F-31400 Toulouse, France
[c] CONICET, Departamento de Geología, Universidad Nacional de Río Cuarto, Campus Universitario, X5804BYA, Río Cuarto, Argentina
[d] Department of Earth and Space Sciences, University of Washington, Box 351310, Seattle, WA 98195, USA

ARTICLE INFO

Article history:
Received 16 November 2021
Received in revised form 17 June 2022
Accepted 1 July 2022
Available online xxxx
Editor: R. Hickey-Vargas

Keywords:
continental evolution
O-Hf/U-Pb isotopes
continental arcs
source contamination
reworking
recycling

ABSTRACT

Since the onset of plate tectonics, continents have evolved through a balance between crustal growth, reworking, and recycling at convergent plate margins. The term "reworking" involves the re-insertion of crustal material into pre-existing crustal volumes, while crustal growth and recycling respectively represent gains from and losses to the mantle. Reworking that occurs in the mantle wedge ("source" contamination from slab material) or within the upper plate ("path" contamination), will have contrasting effects on crustal evolution. However, due to limited access to deep crustal and mantle rocks, quantifying source *vs*. path contamination remains challenging. Based on the 4-dimensional record of the fossil (Ordovician) Famatinian continental arc (Argentina), we demonstrate that source contamination plays a dominant role in imprinting mafic to granitic rocks with crustal oxygen-hafnium (O-Hf) isotopic compositions. We argue that source contamination at convergent plate margins significantly increased the diversity of O-Hf isotopic signatures of continents over geologic time. Our interpretation implies that crustal evolution models attributing this isotopic diversity dominantly to intra-crustal reworking may be over-simplistic and may underestimate continental growth in the last 2.5 billion years.

1. Introduction

The evolution of the volume of continental crust depends on the balance between three mass fluxes (Plank and Langmuir, 1998; Roberts and Spencer, 2015; Stern and Scholl, 2010): (i) **crustal growth** by addition of mantle-derived magmas; (ii) **crustal reworking**, i.e. mass redistribution within the crust; and (iii) **crustal recycling** to the mantle via subduction-related processes and/or delamination. Therefore, understanding the evolution of the continental crust requires quantification of their relative contributions at all spatial and temporal scales (Korenaga, 2018). Convergent margin ("arc") magmatism has been modulating these fluxes since the onset of plate tectonics, i.e. at least for three billion years (Hawkesworth et al., 2020; Rudnick and Gao, 2003). Specifically, three main reservoirs contribute to the production of arc magmas (Hawkesworth et al., 2020; Tatsumi and Kogiso, 2003): (1) the mantle wedge, whose melting results in crustal growth; (2) the slab, including a hydrated oceanic crust and some amount of continent-derived sediments, the latter of which, depending on whether they are incorporated in arc magmas or not, contribute to either recycling or crustal reworking in the form of "source" contamination; and (3) the overriding crust, whose melting contributes to crustal reworking in the form of "path" contamination.

The chemical and isotopic compositions of arc magmas may thus reflect both source contamination of the mantle wedge by slab-derived material; and path contamination of mantle-derived magmas by melting of the overriding crust. These two mechanisms have fundamentally different predictions in terms of the mass and energy balance for the long-term evolution of continents. For a given volume of magma, source contamination is expected to need less crustal material than path contamination to reach a given chemical and isotopic signature (Hawkesworth et al., 1993); and an increase in source contamination also entails a concomitant decrease in crustal recycling (into the mantle) as slab material is re-incorporated to the crust. Distinguishing between the two processes, therefore, is essential for quantifying the balance between

* Corresponding author.
E-mail address: jc.julien.cornet@gmail.com (J. Cornet).

https://doi.org/10.1016/j.epsl.2022.117706

crustal growth, recycling and reworking in arcs and in turn, the interpretation of isotopic proxies used to upscale regional observations to the global scale, such as oxygen (O) and hafnium (Hf) isotopic compositions of detrital zircon (Hawkesworth and Kemp, 2006; Korenaga, 2018; Roberts and Spencer, 2015).

Quantifying the relative importance of source and path contamination in a given arc requires detailed knowledge of end-member compositions for each reservoir, their spatial variations, and the way they may interact in the lower crust and mantle wedge (Jacob et al., 2021; Jagoutz and Klein, 2018). However, such knowledge is generally lacking, as exposure bias skews the study of arc magmatism towards its end products (i.e., upper crustal intermediate to silicic plutons and volcanic rocks). Even in rare areas where arc crustal sections are thoroughly studied, these are represented by former oceanic arcs (e.g., Talkeetna and Kohistan arc, Greene et al., 2006; Jagoutz and Klein, 2018), which, by definition, lack large pre-existing crustal volumes susceptible to interact with the mantle magmas, so that the relative impact of source and path contamination remains poorly understood.

In this paper, we address the problem by focusing on an exceptional natural laboratory, the Famatinian continental arc section. This arc has exposures of large volumes of lower crustal mafic, mid-crustal intermediate, upper crustal silicic plutonic rocks and their host crustal rocks, and the paleogeography of the different magmatic units is well reconstructed (Otamendi et al., 2020; Rapela et al., 2018). Altogether, the Famatinian arc offers the unique opportunity to evaluate the role of source vs. path contamination in a continental arc. We combine bulk-rock petrological data, with an extensive database of high-precision U/Pb ages and in-situ Hf-O isotopic ratios on zircon from all available rock types in the Famatinian system to decipher the contributions of source and path contamination during this Ordovician magmatic episode.

2. Methods

2.1. Major, trace and Ca isotopes bulk rock measurements

We present here bulk-rock data from 73 samples collected from this study that is added to a pre-existing compilation of 310 samples for the Famatinian arc (Camilletti et al., 2020; Walker et al., 2015). Bulk rock major and trace element analyses were collected using XRF methods and are provided in **Supplementary Material 1**. We also present radiogenic Ca isotope measurements performed on 4 endmember samples that span the entire compositional range observed in our collection (Antonelli and Simon, 2020; Supplementary material 6).

2.2. O-Hf isotopes, U-Pb dating and trace elements in zircon

We have investigated a total of 62 samples for zircon geochemistry. Zircon were separated from other phases using a high voltage selective fragmentation apparatus (SelFrag) followed by heavy liquids, magnetic separation and hand picking. Zircon were annealed at 900 °C for 48 h in a muffle furnace before being placed on epoxy mounts together with two reference materials (91500 and Mud-Tank, Ávila et al., 2020; Wiedenbeck et al., 2004) that underwent the same annealing protocol. Zircon grains were imaged using a Deben Centaurus panchromatic cathodoluminescence (CL) detector mounted on a Jeol JSM-6390LA Secondary Electron Microscope (SEM) in ETH Zurich (images available in **Supplementary Material 2**). The images were used to identify potential inherited cores, metamict zones and inclusions. In chronological order, we used Secondary Ion Mass Spectrometry (SIMS) for O isotopes, Laser Ablation Inductively Coupled Plasma Mass Spectrometry (LA-ICPMS) for preliminary U-Pb dating and trace element concentrations, and LA-Multi Collector-ICPMS (LA-MC-ICPMS) for Hf isotopes. A selection of 21 representative samples based on the lack of inherited cores, geographical relevance and data quality from other analytical measurements (e.g., close to average 1 s.d. or, in the case of LA-ICPMS dates, 1 propagated errors) were analyzed for high precision U-Pb geochronology using chemical abrasion - isotope dilution thermal ionization mass spectrometry techniques (CA-ID-TIMS) at ETH Zurich (Wotzlaw et al., 2017). Details about the analytical methods are provided in the supplementary materials. Supplementary Tables 1 to 6 contain the data presented hereafter and the CL images.

3. The anatomy and construction of the Famatinian arc

3.1. Geological background

The activity of the Famatinian arc in Argentina started during the late Cambrian, at ca. 490 Ma, due to the protracted convergence between Gondwana and Laurentia that began during the Pre-Cambrian (Otamendi et al., 2020; Rapela et al., 2018). The Famatinian magmatism was responsible for thickening the crust to 25-30 km with coeval formation of volcano-sedimentary deposits from sub-aerial volcanoes locally named the Suri formation (Armas et al., 2020). The arc magmas intruded into a thin continental crust (ca. 15 km) mainly composed of Cambrian, siliciclastic metasedimentary rocks locally named, from bottom to top, the Negro Peinado formation and the Achavil formation (**Fig. 1**, Collo et al., 2009). These pre-existing crustal components of the upper plate are characterized by a *monotonous* lithological association at the crustal-scale along the arc axis at the time of formation of the Famatinian arc, dominated by turbiditic sequences (Otamendi et al., 2020; Rapela et al., 2018). The Famatinian arc ended with the collision of the Cuyania terrane around 460 Ma ago. This terrane, lying west of the suture zone, is composed of a Proterozoic basement overlain by early Paleozoic sedimentary rocks (Ramacciotti et al., 2015; Thomas and Astini, 2003; Ramos, 2004). These sediments were accreted along the margin of Gondwana in the Ordovician (Ramos, 2004) and partly subducted under the Famatinian arc, as indicated by high-pressure and high-temperature metamorphism (12 kbar, 780 °C, e.g., Mulcahy et al., 2014) and structural evidence of slab entrainment (Ramos, 2004; van Staal et al., 2011).

The most voluminous magmas of the Ordovician Famatinian arc are grouped in three locality types along a ~600 km N-S transect with each of them representing different crustal levels: (1) the lower crust in Valle Fértil (between 30 and 31.5°S) subdivided as a mafic (Walker et al., 2015) and intermediate zone (Camilletti et al., 2020), (2) the intermediate crust in the Sierra de Famatina (between 28.5 and 30°S; Dahlquist et al., 2008), and (3) the upper crust with the Ordovician sub-surface in the Chaschuil belt (between 27 and 28°S; Armas et al., 2020) (**Fig. 1**). The Valle Fértil area shows a large range of mafic to intermediate plutonic rocks that intruded and metamorphosed the local crust at pressure estimated from 8 to 5 kbar by typical mineral assemblages (e.g., garnet-cordierite-sillimanite bearing migmatites, Tibaldi et al., 2013). The Sierra de Famatina batholith grew at pressures equivalent of ca. 5 kbar, which was derived from geological evidence of contacts with both the Negro Peinado and the Achavil formation (Dahlquist et al., 2008), the occurrence of magmatic epidote in plutonic samples and mineral assemblages in the metamorphosed host rock (cordierite-garnet bearing migmatites; Alasino et al., 2014). The Chaschuil belt settled at a pressure lower than 2 kbar, as inferred from the intrusive contact with the overlying sub-surficial volcano-clastic series locally named the Suri formation (Armas et al., 2020). The Chaschuil belt as well as the Sierra de Famatina are marked by the presence of granodioritic periph-

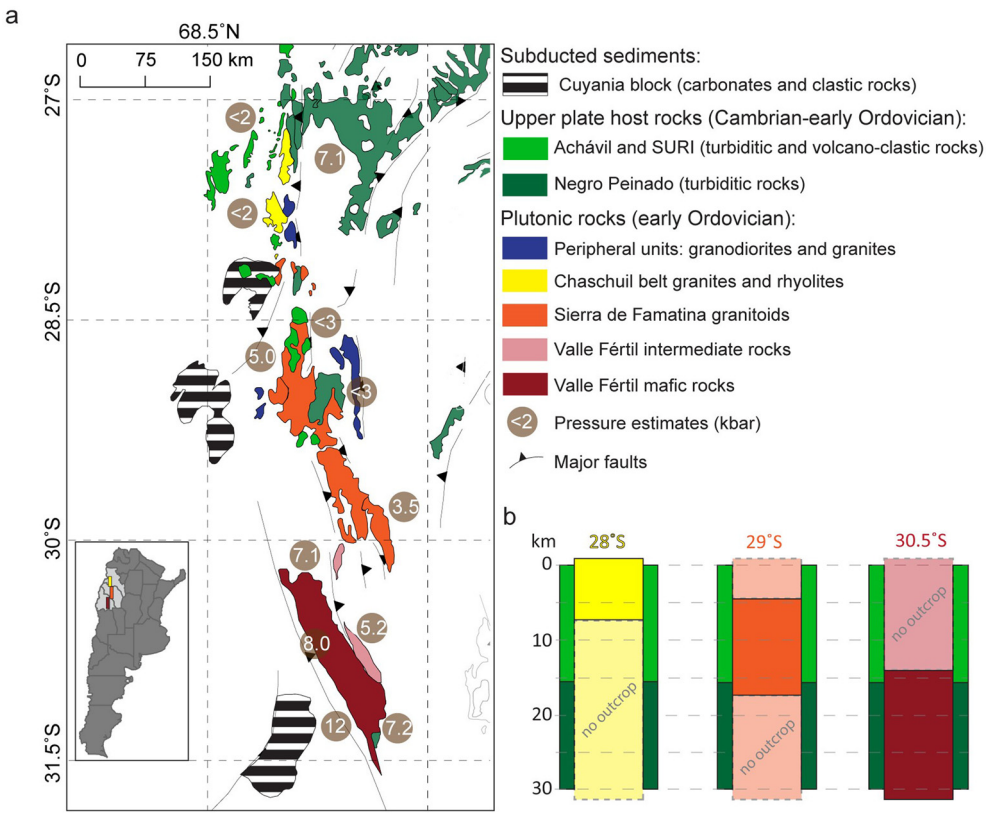

Fig. 1. (a) Geometry of the Famatinian paleo-arc in NW Argentina modified from Otamendi et al. (2020) showing the location of the three magmatic centers, the remnants of subducted sediments from the Cuyania terrane, and the paleo pressures revealing the various crustal depths of exposure for the different magmatic centers. (b) Simplified lithostratigraphic columns resuming the 3D geometry of the different outcrops along the N-S axis that shows that each magmatic center is an individual magmatic column.

eral units outcropping on the edges of the main magmatic centers (**Fig. 1**).

3.2. Geochemical connections

3.2.1. Bulk rocks

In the Mg# [molar$Mg^{2+}/(Mg^{2+} + Fe^{2+})$ with Fe^{2+} as total Fe] vs. SiO_2 diagram, the most mafic rocks (<55 wt.% SiO_2) display a Z-shaped pattern mimicking the composition of cumulates from the fractional crystallization of hydrous and oxidized, primitive arc magmas (**Fig. 2a**; Jagoutz and Klein, 2018; Müntener and Ulmer, 2018). The more silicic rocks define a metaluminous series (Aluminium Saturation Index [ASI] < 1), at the exception of the peripheral units (see below), consistent with olivine-orthopyroxene/clinopyroxene-Fe-Ti oxides-amphibole fractionation in the deep crust and an amphibole-plagioclase dominated differentiation in the mid crust (Camilletti et al., 2020; Otamendi et al., 2020; Walker et al., 2015). The existence of Ordovician peraluminous rocks (ASI > 1; **Fig. 2b**) in the Famatinian arc, likely formed by local anatexis of pre-existing sedimentary rocks (Otamendi et al., 2008; Tibaldi et al., 2013), raises the question of the contribution of crustal melts to the magmatic suite. However, these anatectic granites represent small outcrops in the Valle Fértil lower crustal section that are geographically limited to near hybridization zones between mafic intrusions and pre-existing overriding crust (Otamendi et al., 2008). The compositions of these granites define a trend of increasing ASI with decreasing SiO_2, typical of "S-type" granites (Jacob et al., 2021), opposite to the main trend of metaluminous samples (**Fig. 2b**). Nevertheless, the volumetrically minor rocks of the peripheral units in Chaschuil and Sierra de Famatina seem to fill the gap between the two metaluminous vs. peraluminous trends at ca. 70 wt.% SiO_2 (**Fig. 2b**).

3.2.2. Zircon trace elements

Because plutonic rocks rarely represent liquids, for mafic compositions but also for silicic ones (Cornet et al., 2022 and reference therein), the trace element composition of evolving melts in a differentiating magma is better observed through the trace element composition of minerals (e.g., zircon). We show here that trace element compositions of zircons capture the differentiation of parental mafic magmas across the different crustal levels of the Famatinian arc (**Fig. 3**). The Eu/Eu* vs. Ti plot (**Fig. 3a**) shows a trend of continuously decreasing Ti concentrations with increasingly negative Eu anomalies from gabbro to granite/rhyolite, reflecting crystallization from progressively cooler, more plagioclase-fractionated melts. The zircon Eu anomaly may partly result from low oxygen fugacity during zircon crystallization (Trail et al., 2012) but if this was the only control, the very low Eu^*/Eu_N (<0.1) observed in zircon from intermediate/felsic rocks would correspond to unrealistically low fO_2 ($\Delta NNO < -4$; Trail et al., 2012) compared to what is expected for arc magmas (Kelley and Cottrell, 2009). For other elements, such as U, Th, Y, Lu, Dy, and Hf (**Fig. 3b-d**), the trends mark the increasing control of accessory phases (including zircon) on the incompatible element budget and the increase of the zircon/melt partition coefficients with decreasing temperature as the melts evolve towards more silicic compositions (Claiborne et al., 2017). The Dy vs. Yb/Dy trend reveals that, upon cooling, zircon was a key phase controlling the budget of these elements as zircon preferentially capture heavy rare earth (HREE) over Mid-REE (MREE), which blurs the potential effect of MREE captur-

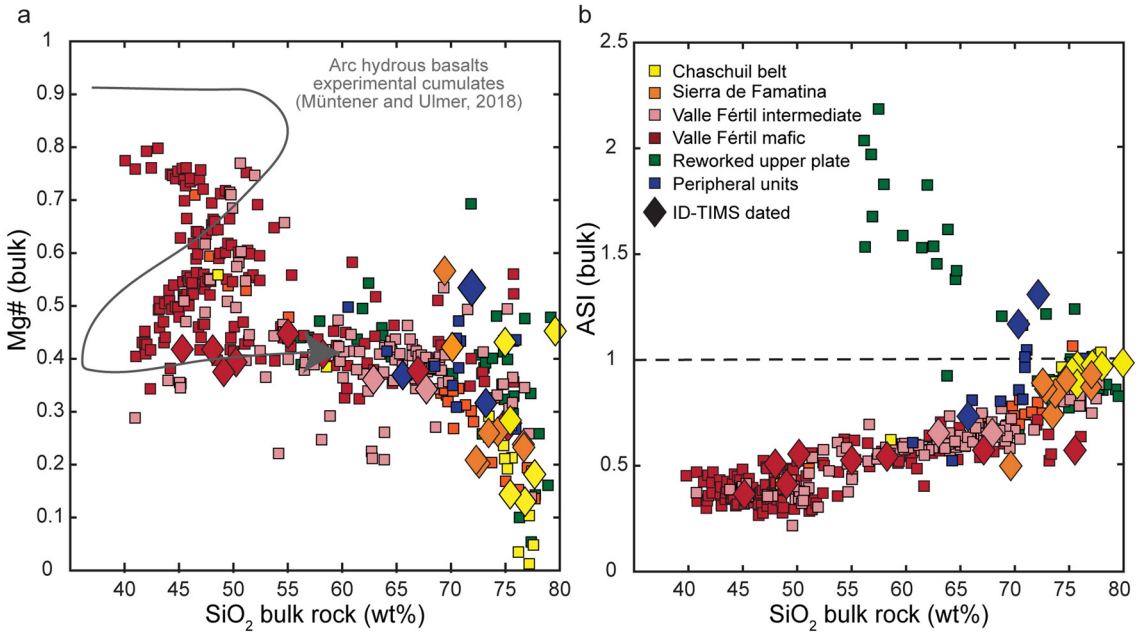

Fig. 2. Bulk-rock geochemical data for the Famatinian Arc samples along the N-S transect. (a) Plot of Mg# [molar Mg/(Mg+Fe)] vs. SiO_2 (wt%) highlighting the continuity between deep-seated mafic cumulates and granites/rhyolites in the Famatinian arc. The data are compared to the general evolution trend (gray arrow) of experimental cumulates from the crystallization of a primary hydrous arc basalt (Müntener and Ulmer, 2018). (b) Plot of Aluminum Saturation Index (ASI) vs. SiO2 (wt%) highlighting the two different, metaluminous and per-aluminous series occurring within the Famatinian arc. The Mg# and the ASI are calculated using the formulation described in **Supplementary Table 1**.

ing phases such as titanite or amphibole and clinopyroxene on the differentiation.

3.3. Geochronological connections

Based on geochronological data, previous studies (Rapela et al., 2018 and references therein) recognized three main magmatic stages in the Famatinian arc: (1) build-up between 491 and 474 Ma; (2) peak magmatism between 474 and 466 Ma; and (3) decline between 466 and 455 Ma. In particular, the peak magmatic stage is well documented from a high-precision (ID-TIMS) U-Pb dataset on a series of samples from the Valle Fértil mafic zone (Ducea et al., 2017). However, there is currently no published high-precision geochronological dataset from samples representing all domains and crustal levels, which prevents a detailed understanding of magmatism at the scale of the entire arc.

We filled this gap by obtaining additional LA-ICP-MS U-Pb dates and isotope dilution thermal ionization mass spectrometry (ID-TIMS) uranium-lead data on 120 single zircon crystals from 21 samples (**Supplementary Table 2-3**). Hereafter, we only discuss magmatic zircon dates. Inherited zircons were absent from the Chaschuil and Sierra de Famatina samples, and only sparsely found in samples from the Valle Fertil area (48 grains out of 194 analyzed by LA-ICP-MS, and 7 out of 18 samples) collected near hybridization zones with the local host rocks (Otamendi et al., 2008). These cores show dominant U-Pb age populations at 1.1–0.9 and 0.6–0.5 Ga, which are typical of detrital zircon from the Negro Peinado formation (Collo et al., 2009).

Zircon dates were used to define estimated probability densities of crystallization ages for each crustal level (**Fig. 4**). Most zircon of the Chaschuil belt and the Sierra de Famatina show ages between 473 and 467 Ma, overlapping the peak magmatic stage defined at 470 ± 3 Ma for Valle Fértil (from this study and Ducea et al., 2017). This shows that the largest magma volumes from ultramafic to highly silicic compositions, along the arc axis and across the exposed transcrustal magmatic column, must have formed in a relatively short magmatic accretion event of 6 million years or less. Importantly, the additional peak at ca. 482 Ma at Chaschuil and samples dated at 478 Ma in the Sierra de Famatina all belong to the peripheral units. We also expect enhanced preservation of zircon from the build-up period in the colder upper and mid-crustal environments relative to the lower crust.

4. Zircon O-Hf systematics

Oxygen (O) and hafnium (Hf) isotopic data for Famatinian arc zircon that crystallized during the peak magmatic event show a counter-intuitive trend. Deep crustal mafic- and cumulate rocks have markedly crustal zircon isotopic compositions with εHf in the range 0 to −5 and $\delta^{18}O_{Zircon}$ between 6.5 and 11.5‰ (corresponding to $\delta^{18}O_{Melt}$ between 8 to 13‰ based on the correction of Bindeman and Valley, 2003). In contrast, mid-/upper crustal intermediate to silicic rocks (both volcanic and plutonic, in the center and north part of the arc) show mantle-like zircon isotopic compositions with εHf in the range 0 to +7 and $\delta^{18}O_{Zircon}$ between 4 and 6.5‰ (corresponding to $\delta^{18}O_{Melt}$ between 5.5 to 8‰) (**Fig. 5a, Supplementary Table 4**). This observation reflects a first-order petrogenetic control on magma production, as it applies to the entire arc and concerns most of the magma volumes produced over its lifetime. The trend could be interpreted in two ways (not mutually exclusive): (i) different amounts of crustal assimilation along the arc (e.g. path contamination/AFC); or (ii) different signatures and/or amounts of crustal components in the mantle source (e.g., source contamination). The respective importance of both processes is discussed in hereafter, notably based on geochemical modeling.

4.1. "Path" contamination and AFC modeling

To perform AFC calculations, we investigated different end-members representing the local host rocks. First, we obtained in-situ O-Hf isotopic analyses directly from Ordovician zircon rims in samples of metasedimentary migmatites embedded in the Valle Fértil mafic zone, representative of partial melts from the local

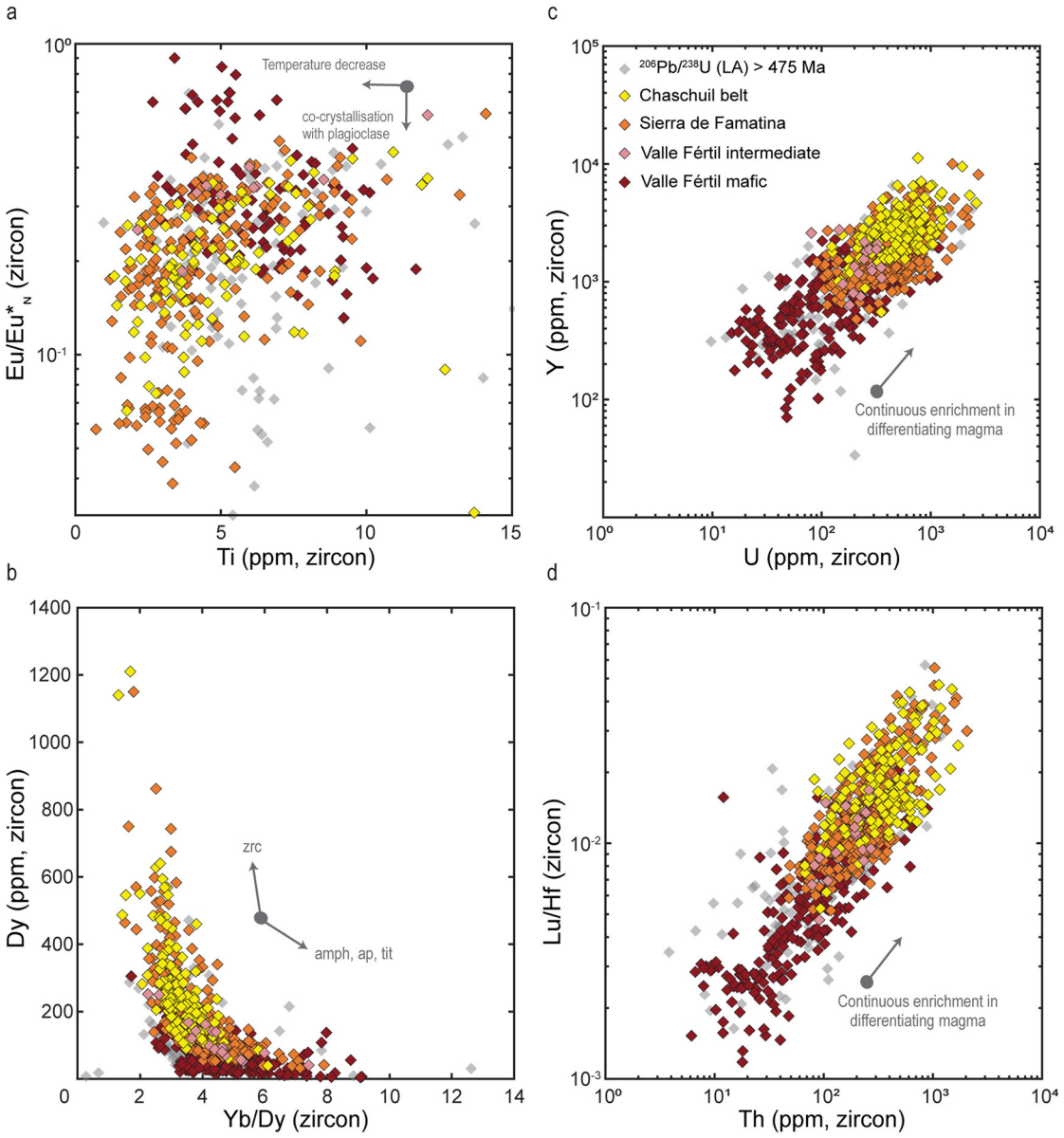

Fig. 3. Zircon trace element geochemistry of the Famatinian plutonic arc samples along the N-S transect excluding the peripheral units. (a) Eu/Eu^*_N vs. Ti highlighting the effect of plagioclase accumulation in a cooling magma prior to zircon saturation. Eu/Eu^*_N normalized to the depleted mantle (Salters and Stracke, 2004), (b) Dy vs. Yb/Dy shows the evolution of mid-Rare Earth (MREE) against Heavy-REE (HREE) and the control of zircon upon the REE budget as the melt temperature decreases and composition evolves towards more silicic. (c) and (d), displaying linear trends of Y vs. U and Lu/Hf vs. Th respectively, show the dominating control of zircon on the budget of these elements and the increase of zircon/melt partition coefficients owing to decreasing temperature and evolving melt composition towards more silicic.

host rocks that interacted with the mafic magmas. Additionally, we have also used bulk-rock Nd isotopic compositions from samples of the Negro Peinado and the Achávil formation obtained in the vicinity of the Valle Fértil and Sierra de Famatina localities to estimate Hf isotopic ratios. The measure εNd range from −7 and −10 (Collo et al., 2009), which translates to εHf = −9.6 to −14.3 (average of −12 used here) using the equation based on the terrestrial array of Vervoort et al. (2011). For oxygen isotopes, we have used $\delta^{18}O$ between 10 and 15‰ which are typical values for paragneiss and pelitic schist (Eiler, 2001) and encompass the $\delta^{18}O$ values we directly obtained on Ordovician zircon rims from the Valle Fértil migmatites (+11 to +13‰). Other possible end-members such as the Puncoviscana formation (Otamendi et al., 2017; Rapela et al., 2018) and other low grade phyllites and schists have isotopic compositions falling in the compositional range used in our calculations. Various D_{Hf} values (from 0.1 to 0.3 as proposed by Kemp et al., 2007) and M_{crust}/M_{magma} values (r-values = 0.2–0.7) are used. We selected the Valle Fértil primitive basalt used by Walker et al. (2015) to estimate the initial Hf concentration of the melt (C_{Hf} = 1.66 ppm). The results of our AFC calculations are shown in **Fig. 5b**.

Deep seated mafic rocks have melt isotopic ratios ($\delta^{18}O$ = 8–10‰, $\varepsilon Hf_{(t)} = -5.0 \pm 0.5$) that are very close to metasedimentary migmatites within the local crust ($\delta^{18}O$ = +11–13‰, $\varepsilon Hf_{(t)} = -5.5 \pm 0.5$). Hence, amounts of assimilation are predicted to be unreasonably high to reach the observed values. In addition, based on AFC modeling (DePaolo, 1981), neither of the selected end-members representing the system **(Fig. 5b)** nor other possible pre-existing crustal end-members (**see Methods; Supplementary Table 5**) show a reasonable fit for the Valle Fértil mafic rocks. Regardless, the closest fitting model would require 25 to 50% fractional crystallization of a Valle Fértil basalt and a high mass ratio of assimilated to crystallized material ("R") of at least ~0.7 (**Fig. 5b, Supplementary Table 5**). Again, the latter is unrealistic in terms

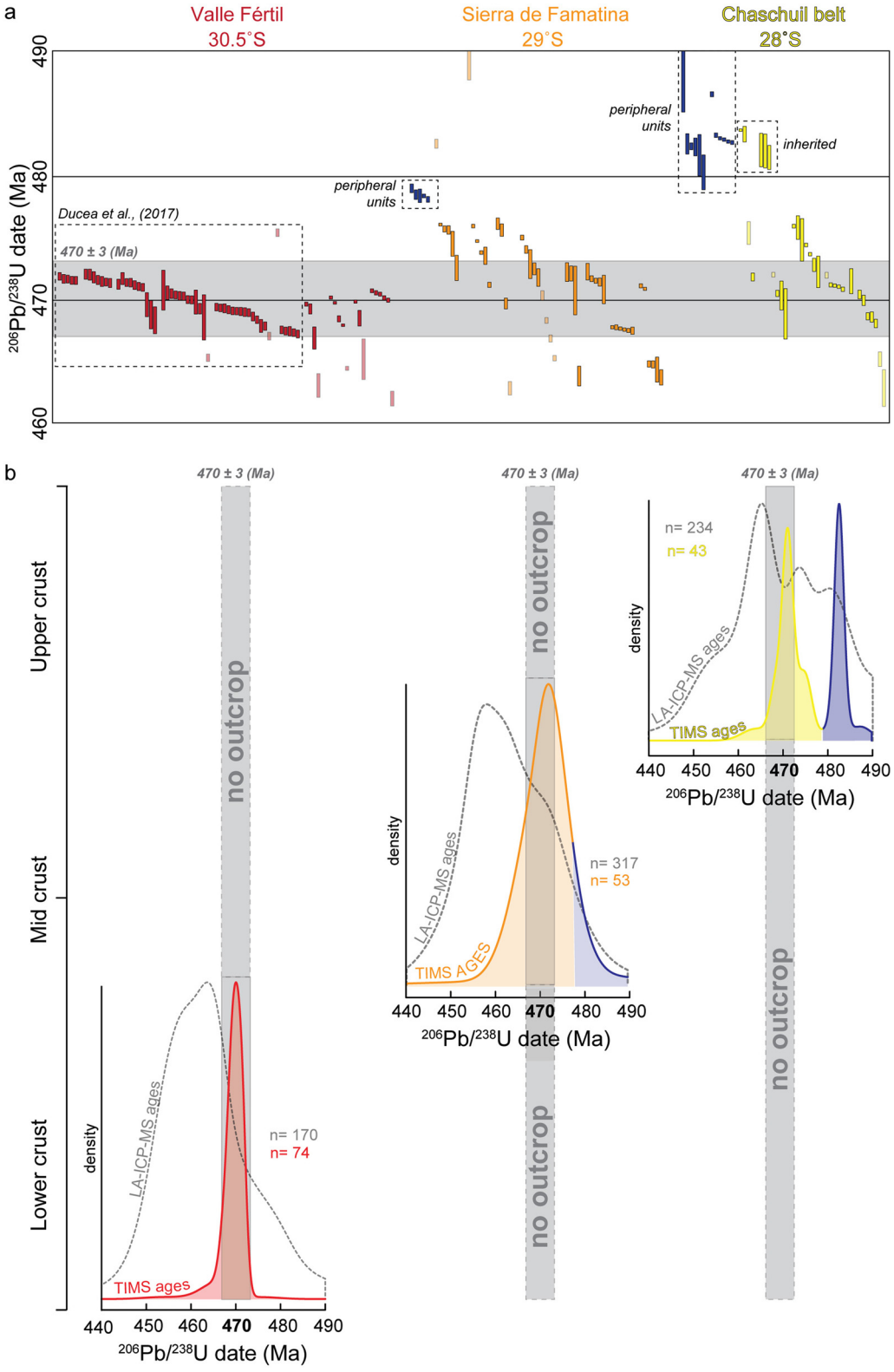

Fig. 4. Summary of geochronological data from the Famatinian arc samples. (a) Individual high-resolution TIMS $^{206}Pb/^{238}U$ zircon dates in Ma measured in this study compiled with the analyses of Ducea et al. (2017) showing the most represented 470 ± 3 Ma ages along the N-S transect. (b) Compilation of estimated probability densities (KDE) for each magmatic center (color coded) and peripheral units (blue). Individual LA-ICP-MS (dashed gray lines) and ID-TIMS (colored lines) dates are reported. The KDEs of individual ID-TIMS dates define the tempo of magma crystallization at the scale of the entire reconstructed crustal column of the Famatinian arc and notably a peak magmatic event at 470 ± 3 Ma (**Supplementary Table 2-3**). KDE of LA-ICP-MS individual dates should be interpreted bearing in mind that the standard error uncertainties are typically 8–15 Ma (2σ) and that the zircon were not chemically abraded prior to analyses. As such, the peak offset and tailing towards younger ages defined by the LA-ICP-MS dates may be a result of significant lead loss.

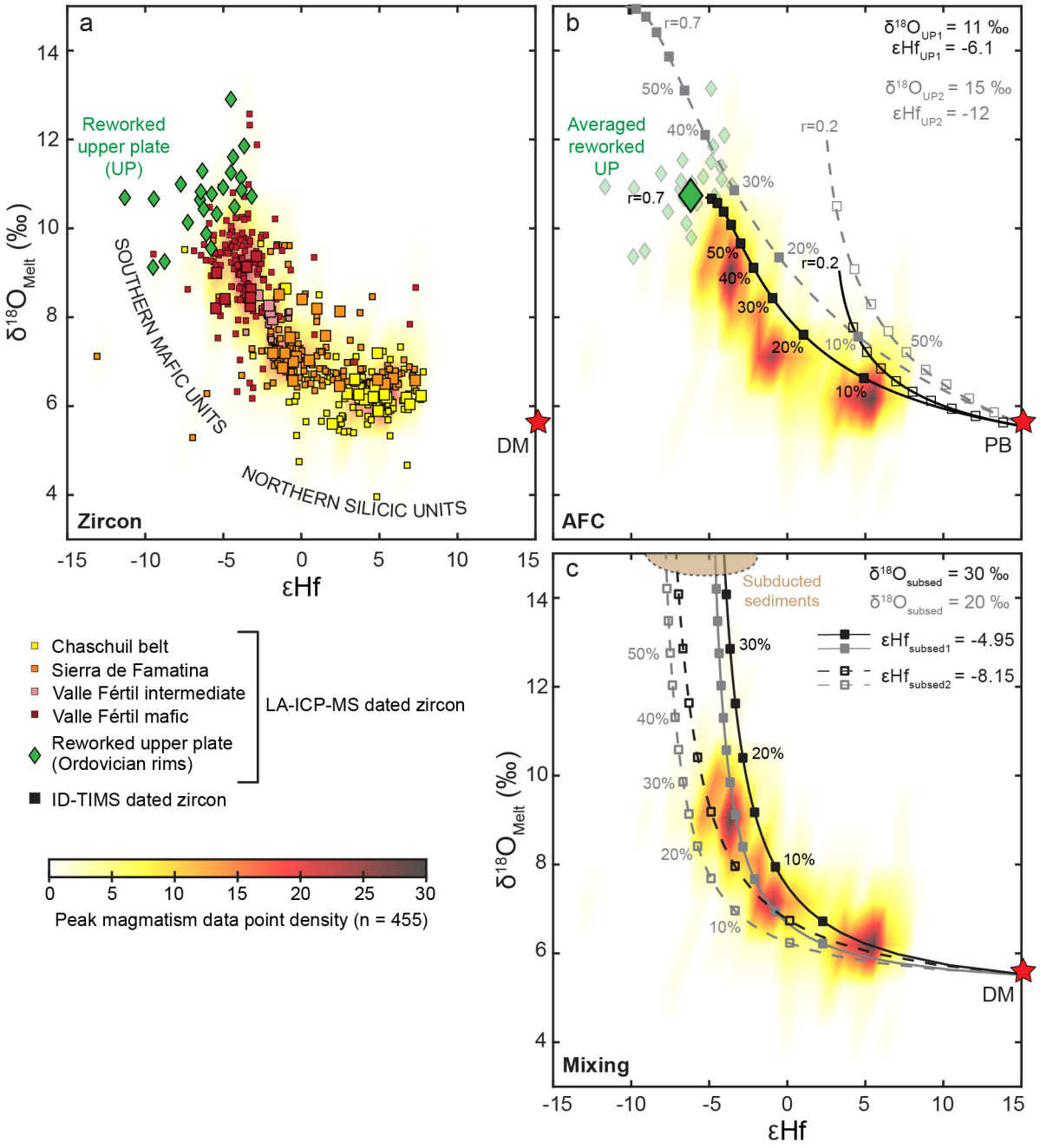

Fig. 5. Crustal signatures in deep mafic rocks, mantle signatures in shallow silicic rocks: the counter-intuitive zircon O-Hf isotopic trend of the Famatinian arc. (a) In-situ O-Hf isotope zircon data for all coeval magmatic samples throughout the peak magmatic event of the Famatinian arc (between 473–467 Ma, **Supplementary Table 4**). Ordovician rims in zircon from metapelite and gneiss constrain the range of compositions for the reworked upper plate. O isotopic compositions are recalculated as those of the zircon-forming melt using the correction factor of Bindeman and Valley (2003) (1.5‰). DM stands for depleted mantle. (b) The range of AFC models used to test the possibility of path contamination to explain the isotopic characteristics of the Famatinian magmas (r = 0.2–0.7, see text). Primitive basalts (PB) differs from the DM because primitive basalts have higher initial Hf concentrations (starting $C_{Hf}^{PB} = 1.66$ ppm, Walker et al., 2015). (c) Mixing models to test source contamination as an explanation for the various isotopic characteristics of Famatinian magmas (see text). Two end-members for εHf are tested: one representing the averaged εHf of the three types of sediments measured (e.g., $\varepsilon Hf_{subsed1}$) by Ramacciotti et al. (2015) and one representing the highest εHf measured in sample SPP-22013 (e.g., $\varepsilon Hf_{subsed2}$) of Ramacciotti et al. (2015). Additional models and model conditions can be found in **Supplementary Table 5**.

of major element compositions of the end products (Walker et al., 2015). An andesitic melt produced by 35% fractionation of a primitive arc basalt (ca. 55 wt.% SiO_2; Ulmer et al., 2018) assimilating a crust-derived granitic melt with >70 wt.% SiO_2 (Otamendi et al., 2009) would result in bulk SiO_2 > 60 wt.% and K_2O of >4 wt.%, rarely observed in the Valle Fértil lower crustal section (**Fig. 2**). Moreover, the AFC models fail to fit the Sierra de Famatina and Chaschuil isotopic composition, and, as the isotopic trend is inversed to what would be expected from conventional AFC, the closest fitting model would create compositions too mafic compared to those observed (e.g., between 65 to 75% of SiO_2, **Fig. 2**).

4.2. "Source" contamination

The sediments of the Cuyania terrane (Ramacciotti et al., 2015), lying west of the suture front with Gondwana (**Fig. 1**), offer the most representative approximation of the $\varepsilon Hf_{(t)}$ of the actual sediment package that subducted underneath the Valle Fértil mag-

matic column, estimated here from bulk-rock εNd data (van Staal et al., 2011) and the equation of Vervoort et al. (2011). Although no O isotopic data exists on these rocks, two distinct δ^{18}O values (+18 and +30 ‰) covering the global range of subducted limestone and schists were used as end-member isotopic compositions (Eiler, 2001; **Supplementary Table 5**). Altogether, these O-Hf isotopic compositions are the most representative end-members of a crustal component that could have interacted with the paleo-mantle wedge at the regional scale. For the mantle end-member, we selected a depleted mantle peridotite with a $C_{Hf} = 0.199$ ppm, $\delta^{18}O = 5.5$‰ and $\varepsilon Hf = 16$.

For the mafic rocks of Valle Fértil, the results of our mixing calculations (**Fig. 5c**) show that the lowest δ^{18}O crustal end-member implies high proportions of sediments in the mixture (up to 40 wt%). However, with the high δ^{18}O end-member, only 15 to 25 wt% of subducted sediment are needed to reproduce the isotopic compositions of Valle Fértil mafic rocks. Given that the Cuyania sequence represents deep-sea sediments (Thomas and Astini, 2003) that have typical δ^{18}O close to or above +30 ‰ (Muehlenbachs, 1998), it is likely that the sediments subducted in this part of the arc had similarly high values. This interpretation is consistent with the results of Spencer et al. (2017) who showed that melting of subducted sediments in the mantle can produce igneous rocks with extremely high δ^{18}O, up to +28‰. Interestingly, the resulting mixing curves also fit well the higher εHf and lower δ^{18}O of zircon-forming melts in Sierra de Famatina and Chaschuil. The proportions, averaging 10% and less than 5% respectively for the two zones exposing shallow crustal Famatinian magmatism, reflect a smaller contribution from sediments than for the deep-seated Valle Fértil magmatism.

5. Discussion

5.1. Building the Famatinian arc magmatic columns from slab to surface

The Famatinian arc is marked by the coeval formation of large granitic batholiths and co-genetic rhyolites (e.g., the Chaschuil belt and parts of the Sierra de Famatina) having mantle-like isotopic signature and a lower crustal magmatic refinery (e.g., Valle Fértil) with crust-like isotopic compositions along a ~600 km N-S arc strike. Such isotopic trends have been interpreted to result from the mixing between mantle basalts and the pre-existing host rocks, especially for the Valle Fértil area, based notably on whole-rock Sm-Nd, Rb-Sr and zircon Lu-Hf isotopes (Otamendi et al., 2017). However, we show here that Valle Fértil mafic rocks have zircon δ^{18}O values similar to those of the host rocks (e.g., zircon rims from the local migmatites and metapelites; literature values of pristine host rocks, **Fig. 5**). Considering a scenario of mixing between mantle-derived basalts and melts from the pre-existing crust, these δ^{18}O values of the zircons in the mafic rock imply that zircons would have crystallized almost entirely from the crustal melts. Such scenario seems highly unlikely as keeping at the same time the bulk rock composition mafic (e.g., analyzed samples are from norites to tonalites, see Supplementary Table 1) and having zircons formed only from small proportions of incorporated crustal melt would imply that this incorporation took place late during crystallization, at crystallinities much above the rheological lock-up threshold (preventing any possible mixing with silicic magmas). Furthermore, the zircon trace element contents in the Valle Fértil samples are typical of those of mafic magmas and belong to a coherent differentiation trend from mafic to silicic magmas, ruling out abundant path contamination as a controlling process (**Fig. 2**). Therefore, we argue here for the contamination of the mantle source by subducting sediments as the main process controlling the isotopic compositions of magmas (and zircon) in Valle Fértil. This source contamination can be traced up to the more silicic lithologies sitting on top of the Valle Fértil mafic zone (Otamendi et al., 2017). Although it was suggested that these evolved rocks were formed through mixing host rock melts and mantle magmas, they have εHf ranging between −8 and −1 which are indiscernible from the Hf signature of the deeper mafic samples.

Assuming that the zircon O-Hf isotopic variation observed at the scale of the entire arc results only from path contamination, the observed trend would require a drastic change of the proportion of assimilated to crystallized material along the arc axis. However, the Famatinian arc magmas were emplaced in compositionally *monotonous* country rocks along the entire arc segment (**Fig. 1**), follow a similar liquid line of descent (**Figs. 2–3**), and were emplaced over a relatively short time interval (**Fig. 4**), precluding significant lateral variations in path contamination. Additionally, mantle-like initial radiogenic ^{40}Ca isotope values measured for a small suite of samples (n = 4) spanning the range of compositions found in the 3 magmatic localities also indicate that the host rock did not play a major role in the building of the main magmatic pulse (**see supplementary Table 6**, and Antonelli and Simon, 2020). We stress that our case for source contamination does not preclude ***some*** path contamination, particularly for the older peripheral units dated at ca. 480 Ma in Chaschuil and the Sierra de Famatina (**Figs. 2–4**); and some magmas from Valle Fertil containing a few inherited zircons (**Fig. 4, Supplementary Material 4**). We note that the older plutonic samples from the peripheral units in Chaschuil and the Sierra de Famatina fall on an alternate trend in the Mg# and ASI vs. SiO_2 diagram (**Fig. 2**), potentially indicating more significant interactions with the pre-existing host rocks. As such, we argue that this slightly older pulse may have partially shielded the mantle-derived magmas of the subsequent peak event from further interactions with pre-existing host rock (Storck et al., 2020).

In lights of our results, we argue for an alternative to the common view that considers assimilation of pre-existing crust en-route to the surface (i.e., path contamination) as the primary origin of chemical and isotopic diversity in arc magmas, (Hawkesworth and Kemp, 2006; Kemp et al., 2007; Spencer et al., 2022). Instead, we consider as equally likely the view of a magmatic column built from distilling mantle magmas, whereby the involvement of older crust, if any, happens through contamination of the mantle source, i.e., source contamination. These magmas evolve within a lower crustal mafic mush reservoir (e.g., the Valle Fértil mafic zone, **Figs. 2–3**) where from the residual andesitic liquids rise upwards to form mid- to upper crustal reservoirs (e.g., the Valle Fértil intermediate zone and Sierra de Famatina) (Bachmann and Huber, 2016 and reference therein). Depending on the thermal regime of the system that is tied to the mantle flux (Karakas et al., 2017), upper crustal granites and rhyolites may form (e.g., the Chaschuil belt) by extraction of highly differentiated liquids (Cornet et al., 2022 and reference therein).

The proposed dominant role of source contamination in shaping the zircon O-Hf isotopic trend of the Famatinian arc implies significant variations in along-arc-strike proportions of subducted sediments contaminating the mantle source (**Fig. 5c**). This means that either the amount of subducted sediments or their contribution to mantle contamination changed along strike of the paleo-subduction zone, owing to different thermo-mechanical regimes along the slab. Paleogeographical models of Otamendi et al. (2020 and references therein) propose that the Cuyania terrane sediments (representative of the paleo-subducted sediments) thin towards the North, and virtually disappear at 28.3°S (Ramos, 2004). This would possibly indicate that the slab below the Chaschuil belt (**Fig. 1**) was practically devoid of sediments. At this northern location, the slab end-member would be dominated by fluids from altered mafic rocks with δ^{18}O much closer to mantle values (+3.5–+6.0‰; e.g., Miller et al., 2001). Altogether, the variation in

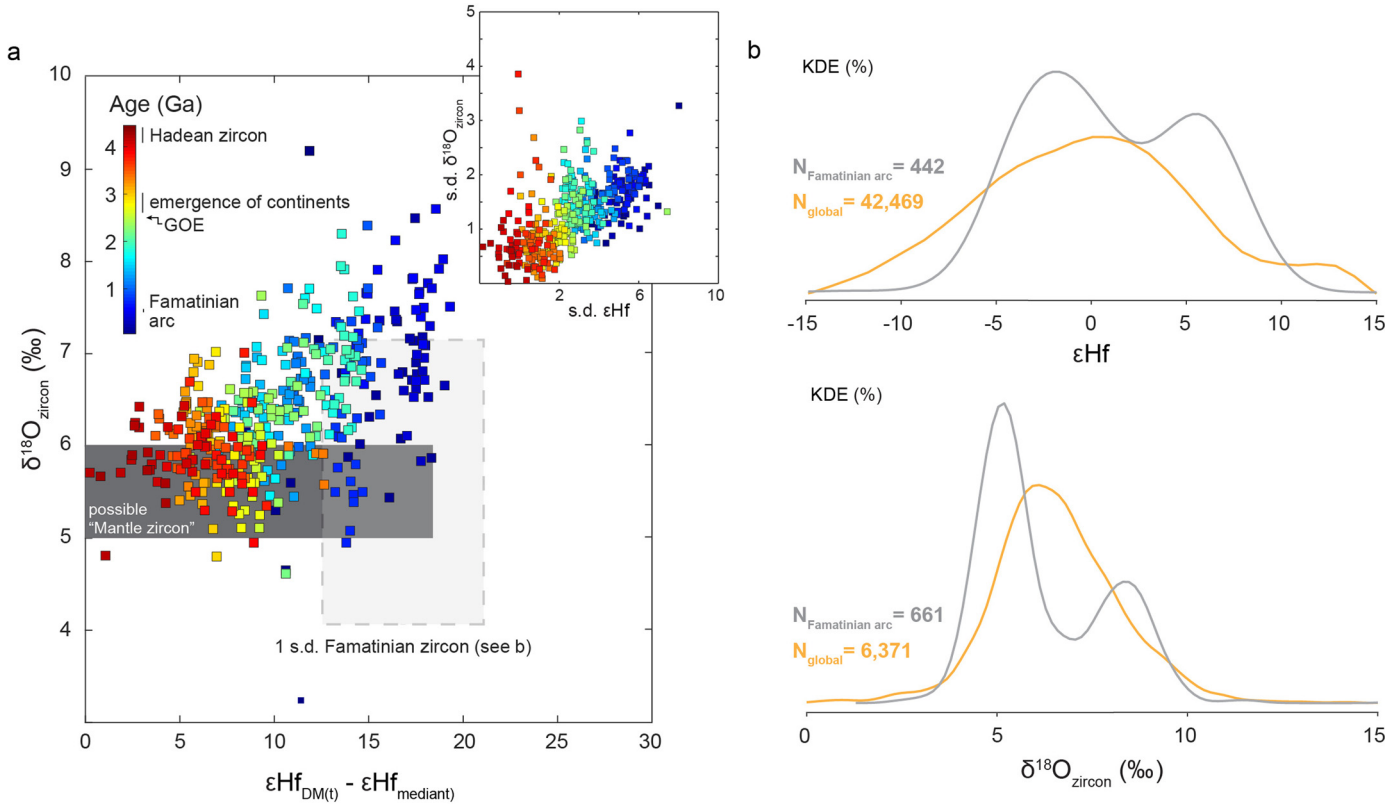

Fig. 6. (a) Median O-Hf isotopic database (Puetz et al., 2021; Spencer et al., 2022) color-coded by age plotted with the range of compositions of the Famatinian arc shown as ±1 standard deviation (s.d.) on the $\delta^{18}O$ and εHf datasets. A median was calculated for every 10 Ma to allow plotting of the O and Hf isotopic signal against one another. $\delta^{18}O$ shows uncorrected for melt zircon data. εHf medians are shown as the distance from the variable depleted mantle Hf value over time (Vervoort and Blichert-Toft, 1999) and is written as $\varepsilon Hf_{DM(t)} - \varepsilon Hf_{median(t)}$. The dark gray box indicates the possible range of "mantle zircon" through time (CHUR < possible mantle zircon < $DM_{(t)}$). The inset displays the evolution of the s.d. on the $\delta^{18}O$ and εHf databases showing the coherent increase of the scatter, and so *the isotopic diversity*, through time. (b) Kernel Density Estimations on the probability of occurrence (%) of each $\delta^{18}O$ and εHf compositions on the databases and the Famatinian dataset. The two KDE reveal the similarity between our dataset and the database suggesting that source contamination controls the isotopic diversification of continental materials through processes resumed in **Fig. 7**.

subducted sediment thickness from south to north is a plausible explanation for the observed counter-intuitive O-Hf isotopic trend.

The process of how slab and subducting sediments fluids/melts enrich the overlying mantle wedge, and the proportion in which it varies along the arc strike, remains elusive. In an arc context, enriching a mantle source could take two forms: either (i) by partial melting of metasedimentary diapirs rising through the asthenospheric wedge (Marschall and Schumacher, 2012) or (ii) by destabilizing the hydrothermally altered layer of the subducting oceanic crust and the overlying sediments at >5 GPa, inducing the release of supercritical fluids (Ni et al., 2017). The maximum amount of contamination to keep the composition of an arc basalt should not exceed 20–25%, which are the maximum values inferred from our results on Valle Fértil (**Fig. 5c**). Therefore, supercritical fluids could have played a role as they resemble a melt enriched with volatile elements (30–70 wt% H_2O, Ni et al., 2017) that are able to scavenge large quantities of usually immobile elements (such as hafnium, Kessel et al., 2005). Therefore, it can be speculated that the source magmas of Valle Fértil could have been contaminated by supercritical fluids, able to change the isotopic composition of the primary arc magmas without drastically changing its major element composition.

5.2. Implications for the global O-Hf record and continental crust evolution

The global zircon record is characterized by an increasing diversity of O-Hf isotopic compositions with time. Specifically, after the onset of plate tectonics and the emergence of subaerial landmasses exposed to erosion ca. 3.0 to 2.5 Ga ago (Bindeman et al., 2018; Hawkesworth et al., 2020; Laurent et al., 2014), zircon shows *both* more scattered O-Hf isotopic compositions and, on average, higher $\delta^{18}O$ and lower εHf than Hadean-Archean zircon (**Fig. 6a and inset**). As newly grown crust is thought to show strongly positive, DM-like Hf isotopic compositions (Dhuime et al., 2011), zircon with lower εHf would reflect a contribution of pre-existing crust, possibly sediment-bearing whenever zircon shows elevated $\delta^{18}O$ (Hawkesworth and Kemp, 2006). Therefore, these secular trends in zircon O-Hf isotopic composition have been commonly interpreted to reflect an increasingly important role of crustal melting over time, i.e. magma production via melting of sediment-bearing, thickened crust in collisional orogenic systems (Hawkesworth et al., 2010; Lackey et al., 2008). This served as a basis for models of crustal evolution, in which the timing of crustal growth is constrained by zircon Hf model ages (Belousova et al., 2010; Dhuime et al., 2012; Korenaga, 2018).

However, we demonstrate here that zircon from the peak magmatic event of a single arc, formed over less than 6 Ma, encompass a zircon O-Hf isotopic variability comparable to that of the global zircon record in the last 2.5 billion years (**Fig. 6b**). In the case of the Famatinian arc, this isotopic diversity was generated mainly through source contamination and with limited (ca. 5–25%) amounts of sedimentary material mixed with the mantle source. The Famatinian arc is unlikely to represent an isolated case, as magmas from several other convergent margin systems, including modern subduction zones (Lesser Antilles, e.g., Davidson, 1983; Sunda-Bunda arc; e.g., Gertisser et al., 2012; Aegean arc, Klaver et al., 2015) as well as older arcs (Roberts et al., 2013) orogenic belts (e.g., Couzinié et al., 2016) and even ophiolites (Spencer et

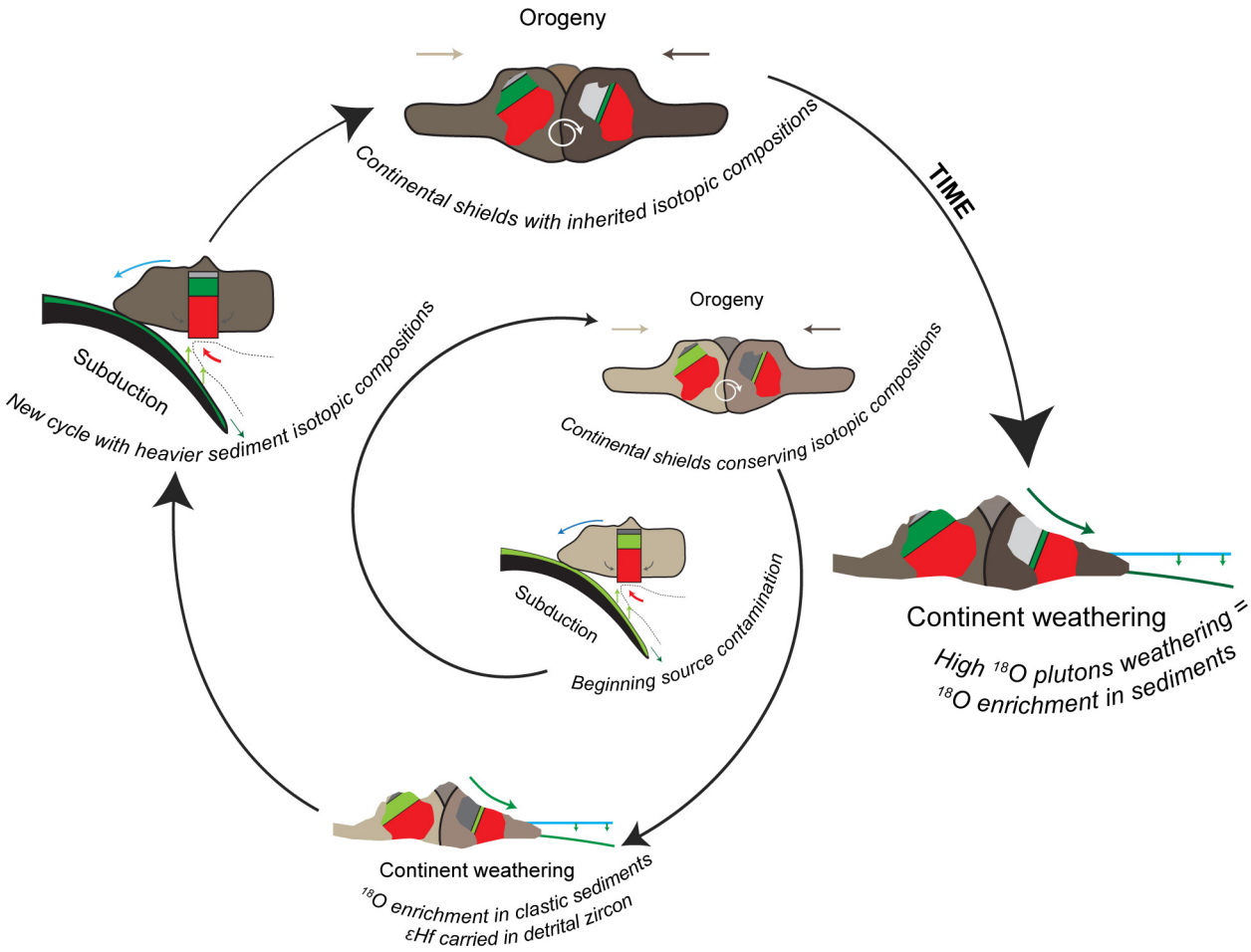

Fig. 7. Synoptic diagram the mechanisms of amplification of the O-Hf isotopic scatter by carrying heavier, "crust-like", O and Hf isotopic compositions in each iteration of orogenic cycles.

al., 2017) also show variations in isotopic signatures that are controlled by source contamination. All combined, this indicates that the isotopic diversity of the global <2.5 Ga-old zircon database must be significantly impacted by reworking of subducted sediments in the source of mantle-derived, convergent margin magmas, i.e., source contamination.

This interpretation is supported by the amplification of the O-Hf scatter and a trend towards heavier averaged O isotope compositions since ~2.5 Ga ago. Indeed, if arc magmas are the main building blocks of continents (Rudnick and Gao, 2003) and hence the main source of clastic sediments, these sediments (and in turn the magmas they contaminate during the subduction cycle) will lead to a progressive increase in $\delta^{18}O$ of igneous rock samples over the course of geologic time (**Fig. 7**). Similarly, the radiogenic Hf isotopic record is expected to scatter more and more with time, as parts of the mantle become increasingly depleted (hence more positive in εHf), while in others, less radiogenic material can be assimilated (hence more negative in εHf), in variable proportions.

Overlooking the importance of source contamination has likely skewed global crust evolution models towards an under-estimation of crustal growth over the past 2.5 Ga, for two main reasons.

1. Some arc igneous rocks, contaminated at their mantle source by small amounts of sediments (as is the case for the Famatinian arc) may show "non-DM-like" zircon O-Hf signatures ($\delta^{18}O > +6.5‰$; $\varepsilon Hf < \varepsilon Hf_{DM}$), although they represent net crustal growth at their crystallization age (i.e. formed by >80% of mantle-derived material by mass; see also Couzinié et al., 2016). These would be typically attributed to crustal reworking in global models, and in turn incorrectly assigned to "ancient" crust formation (i.e. given by zircon Hf model ages) instead of "instantaneous" growth (i.e. given by zircon U-Pb ages) (Belousova et al., 2010; Dhuime et al., 2012; Roberts and Spencer, 2015).
2. Source contamination means that some fraction of reworked crust (in the form of sediments originating from weathering of arc magmas, Plank and Langmuir, 1998) is withdrawn from the slab and does not undergo recycling into the deeper mantle. This effect, generally not considered in the global balance between crustal growth and recycling (Scholl and von Huene, 2009; Stern and Scholl, 2010), could be non-negligible. For example, the Famatinian arc has between 5 and 25% by mass of sediment addition during the peak magmatic event, with a total magma flux of ca. 250–300 $km^3.km^{-1}.Ma^{-1}$ (Otamendi et al., 2020; Ducea et al., 2017). This translates into a flux of subducted sediments returning to the continental crust of 13 to 75 $km^3.km^{-1}.Ma^{-1}$, clearly significant in light of the global, average subducted sediment flux (60 $km^3.km^{-1}.Ma^{-1}$; Scholl and von Huene, 2009). Therefore, the interpretation that, in the context of modern plate tectonics, crustal growth being balanced or even outpaced by recycling (Scholl and von Huene, 2009), should be reconsidered.

6. Conclusion

The geological processes recorded in 4-D in the Famatinian arc provides a unique window into the shaping of Earth's continental crust. Our results, supported by the geological layout of the area,

provide compelling evidence for the building of continental arc magmatic columns from coeval fractionating mantle-derived mafic magmas. However, systematic variations in zircon O-Hf isotopic compositions of the Famatinian arc magmas are best explained by the variable incorporation of crustal material from subducted sediments along the N-S arc strike, hence revealing the key role of source contamination. By comparing our zircon isotopic data with O-Hf databases, we suggest that the addition of subducted sediments in magmas of arcs has been playing a non-negligible role in the global, secular isotopic trends shown by the continental crust (**Figs. 6–7**). We do not exclude the role of other mechanisms, such as assimilation of the overriding plate ("path" contamination) and partial melting during collision and post-collisional stages (Moyen et al., 2021 and references therein). However, we emphasize here that the contribution of subducted sediments to arc magmas has the potential to (i) primarily generate the isotopic diversity typically attributed to path contamination; and (ii) conceal recent crustal growth, leading to overestimates of both crustal reworking and recycling through geologic time.

CRediT authorship contribution statement

Julien Cornet was responsible of sample collection, processing, interpretation and writing of the article in the frame of his PhD thesis.

M. Antonelli provided with Ca isotopes measurements.

O. Laurent and J.-F. Wotzlaw helped analyzing and processing the zircon data (LAICPMS and TIMS, respectively).

O. Laurent helped analyzing and processing the Hf isotopes.

J. Otamendi was the field head in Argentina.

G.W. Bergantz analyzed (through Barry A Walker and Chad Deering) O-isotopes in the Valle Fértil zircon and provided with Valle Fértil samples.

O. Bachmann and J. Otamendi are the designers of the project.

All authors contributed to the interpretation of data and editing of the manuscript.

Declaration of competing interest

The authors declare that they have no known competing financial interests or personal relationships that could have appeared to influence the work reported in this paper.

Acknowledgements

We thank Chris Spencer as well as 3 anonymous reviewers for their constructive comments to improve the quality of this paper. This study was supported by the Swiss-Argentinian SNF grant IZSAZ2_173428. We warmly thank Andrea Galli, Matthieu Galvez, Facundo Escribano, Giuliano Camilletti, Eber Cristofolini, Matías Barzola, Alina Fiedrich for discussions as well as Fabrizio, Fabian and Roque for their technical support in the remote field areas. Barry A Walker and Chad Deering helped with sample preparation and the analysis of oxygen isotopes in zircon from the mafic complex of Valle Fértil at the WiscSIMS (funded by National Science Grant EAR-1049884 to George W. Bergantz). The WiscSIMS is supported by the US National Science Foundation (NSF) (EAR-1658823) and the University of Wisconsin-Madison.

Appendix A. Supplementary material

Supplementary material related to this article can be found online at https://doi.org/10.1016/j.epsl.2022.117706.

References

Alasino, P.H., Casquet, C., Larrovere, M.A., Pankhurst, R.J., Galindo, C., Dahlquist, J.A., Baldo, E.G., Rapela, C.W., 2014. The evolution of a mid-crustal thermal aureole at Cerro Toro, Sierra de Famatina, NW Argentina. Lithos 190–191, 154–172. https://doi.org/10.1016/j.lithos.2013.12.006.

Antonelli, M.A., Simon, J.I., 2020. Calcium isotopes in high-temperature terrestrial processes. Chem. Geol. 548, 119651. https://doi.org/10.1016/j.chemgeo.2020.119651.

Armas, P., Cristofolini, E., Escribano, F., Camilletti, G., Barzola, M., Otamendi, J., Cisterna, C., Leisen, M., Romero, R., Barra, F., Tibaldi, A., 2020. Lower-middle ordovician sedimentary environment and provenance of the suri formation in the northern region of the Famatina belt, Catamarca, Argentina. J. South Am. Earth Sci. 102948. https://doi.org/10.1016/j.jsames.2020.102948.

Ávila, J.N., Ireland, T.R., Holden, P., Lanc, P., Latimore, A., Schram, N., Foster, J., Williams, I.S., Loiselle, L., Fu, B., 2020. High-precision, high-accuracy oxygen isotope measurements of zircon reference materials with the SHRIMP-SI. Geostand. Geoanal. Res. 44 (1), 85–102. https://doi.org/10.1111/ggr.12298.

Bachmann, O., Huber, C., 2016. Silicic magma reservoirs in the Earth's crust. Am. Mineral. 101 (11), 2377–2404. https://doi.org/10.2138/am-2016-5675. GeoScienceWorld.

Belousova, E.A., Kostitsyn, Y.A., Griffin, W.L., Begg, G.C., O'Reilly, S.Y., Pearson, N.J., 2010. The growth of the continental crust: constraints from zircon Hf-isotope data. Lithos 119 (3–4), 457–466. https://doi.org/10.1016/j.lithos.2010.07.024.

Bindeman, I.N., Valley, J.W., 2003. Rapid generation of both high- and low-δ18O, large-volume silicic magmas at the Timber Mountain/Oasis Valley caldera complex, Nevada. Bull. Geol. Soc. Am. 115 (5), 581–595. https://doi.org/10.1130/0016-7606(2003)115<0581:RGOBHA>2.0.CO;2.

Bindeman, I.N., Zakharov, D.O., Palandri, J., Greber, N.D., Dauphas, N., Retallack, G.J., Hofmann, A., Lackey, J.S., Bekker, A., 2018. Rapid emergence of subaerial landmasses and onset of a modern hydrologic cycle 2.5 billion years ago. Nature 557 (7706), 545–548. https://doi.org/10.1038/s41586-018-0131-1.

Camilletti, G., Otamendi, J., Tibaldi, A., Cristofolini, E., Leisen, M., Romero, R., Barra, F., Armas, P., Barzola, M., 2020. Geology, petrology and geochronology of sierra Valle Fértil - La Huerta batholith: implications for the construction of a middle-crust magmatic-arc section. J. South Am. Earth Sci. 97, 102423. https://doi.org/10.1016/j.jsames.2019.102423.

Claiborne, L.L., Miller, C.F., Gualda, G.A.R., Carley, T.L., Covey, A.K., Wooden, J.L., Fleming, M.A., 2017. Zircon as magma monitor. In: Microstructural Geochronology: Planetary Records Down to Atom Scale, pp. 1–33.

Collo, G., Astini, R.A., Cawood, P.A., Buchan, C., Pimentel, M., 2009. U-Pb detrital zircon ages and Sm-Nd isotopic features in low-grade metasedimentary rocks of the Famatina belt: implications for late Neoproterozoic-early Palaeozoic evolution of the proto-Andean margin of Gondwana. J. Geol. Soc. 166 (2), 303–319. https://doi.org/10.1144/0016-76492008-051.

Cornet, J., Bachmann, O., Ganne, J., Fiedrich, A., Huber, C., Deering, C.D., Feng, X., 2022. Assessing the effect of melt extraction from mushy reservoirs on compositions of granitoids: from a global database to a single batholith. Geosphere 18 (3). https://doi.org/10.1130/ges02333.1.

Couzinié, S., Laurent, O., Moyen, J.F., Zeh, A., Bouilhol, P., Villaros, A., 2016. Post-collisional magmatism: crustal growth not identified by zircon Hf–O isotopes. Earth Planet. Sci. Lett. 456, 182–195. https://doi.org/10.1016/j.epsl.2016.09.033.

Dahlquist, J.A., Pankhurst, R.J., Rapela, C.W., Galindo, C., Alasino, P., Fanning, C.M., Saavedra, J., Baldo, E., 2008. New SHRIMP U-Pb data from the Famatina Complex: constraining Early-Mid Ordovician Famatinian magmatism in the Sierras Pampeanas, Argentina. Geol. Acta 6 (4), 319–333. https://doi.org/10.1344/105.000000260.

Davidson, J.P., 1983. Lesser Antilles isotopic evidence of the role of subducted sediment in island arc magma genesis. Nature 306 (5940), 253–256. https://doi.org/10.1038/306253a0.

DePaolo, D.J., 1981. Trace element and isotopic effects of combined wallrock assimilation and fractional crystallization. Earth Planet. Sci. Lett. 53 (2), 189–202. https://doi.org/10.1016/0012-821X(81)90153-9.

Dhuime, B., Hawkesworth, C.J., Cawood, P.A., 2011. When continents formed. Science 331 (6014), 154–155. https://doi.org/10.1126/science.1201245.

Dhuime, B., Hawkesworth, C.J., Cawood, P.A., Storey, C.D., 2012. A change in the geodynamics of continental growth 3 billion years ago. Science 335 (6074), 1334–1336. https://doi.org/10.1126/science.1216066.

Ducea, M.N., Bergantz, G.W., Crowley, J.L., Otamendi, J., 2017. Ultrafast magmatic buildup and diversification to produce continental crust during subduction. Geology 45 (3), 235–238. https://doi.org/10.1130/G38726.1.

Eiler, J.M., 2001. Oxygen isotope variations of basaltic lavas and upper mantle rocks. Rev. Mineral. Geochem. 43 (1), 319–364. https://doi.org/10.2138/gsrmg.43.1.319.

Gertisser, R., Self, S., Thomas, L.L., Handley, H.K., Van Calsteren, P., Wolff, J.A., 2012. Processes and timescales of magma genesis and differentiation leading to the great tambora eruption in 1815. J. Petrol. 53 (2), 271–297. https://doi.org/10.1093/petrology/egr062.

Greene, A.R., DeBari, S.M., Kelemen, P.B., Blusztajn, J., Clift, P.D., 2006. A detailed geochemical study of island arc crust: the Talkeetna arc section, south–central Alaska. J. Petrol. 47 (6), 1051–1093. https://doi.org/10.1093/petrology/egl002.

Hawkesworth, C.J., Cawood, P.A., Dhuime, B., 2020. The Evolution of the Continental Crust and the Onset of Plate Tectonics. Frontiers in Earth Science, vol. 8. Frontiers Media S.A.

Hawkesworth, C.J., Dhuime, B., Pietranik, A.B., Cawood, P.A., Kemp, A.I.S., Storey, C.D., 2010. The generation and evolution of the continental crust. J. Geol. Soc. 167 (2), 229–248. https://doi.org/10.1144/0016-76492009-072. Geological Society of London.

Hawkesworth, C.J., Gallagher, K., Hergt, J.M., McDermott, F., 1993. Mantle and slab contributions in arc magmas. Annu. Rev. Earth Planet. Sci. 21, 175–204. https://doi.org/10.1146/annurev.ea.21.050193.001135.

Hawkesworth, C.J., Kemp, A.I.S., 2006. Using hafnium and oxygen isotopes in zircons to unravel the record of crustal evolution. Chem. Geol. 226 (3–4), 144–162. https://doi.org/10.1016/j.chemgeo.2005.09.018.

Jacob, J.B., Moyen, J.F., Fiannacca, P., Laurent, O., Bachmann, O., Janoušek, V., Farina, F., Villaros, A., 2021. Crustal melting vs. fractionation of basaltic magmas: part 2, attempting to quantify mantle and crustal contributions in granitoids. Lithos 402–403, 106292. https://doi.org/10.1016/J.LITHOS.2021.106292.

Jagoutz, O., Klein, B., 2018. On the importance of crystallization-differentiation for the generation of SiO2-rich melts and the compositional build-up of ARC (and continental) crust. Am. J. Sci. 318 (1), 29–63. https://doi.org/10.2475/01.2018.03.

Karakas, O., Degruyter, W., Bachmann, O., Dufek, J., 2017. Lifetime and size of shallow magma bodies controlled by crustal-scale magmatism. Nat. Geosci. 10 (6), 446–450. https://doi.org/10.1038/ngeo2959.

Kelley, K.A., Cottrell, E., 2009. Water and the oxidation state of subduction zone magmas. Science 325 (5940), 605–607. https://doi.org/10.1126/science.1174156.

Kemp, A.I.S., Hawkesworth, C.J., Foster, G.L., Paterson, B.A., Woodhead, J.D., Hergt, J.M., Gray, C.M., Whitehouse, M.J., 2007. Magmatic and crustal differentiation history of granitic rocks from Hf-O isotopes in zircon. Science 315 (5814), 980–983. https://doi.org/10.1126/science.1136154.

Kessel, R., Schmidt, M.W., Ulmer, P., Pettke, T., 2005. Trace element signature of subduction-zone fluids, melts and supercritical liquids at 120–180 km depth. Nature 437 (7059), 724–727. https://doi.org/10.1038/nature03971.

Klaver, M., Djuly, T., de Graaf, S., Sakes, A., Wijbrans, J., Davies, G., Vroon, P., 2015. Temporal and spatial variations in provenance of Eastern Mediterranean Sea sediments: Implications for Aegean and Aeolian arc volcanism. Geochim. Cosmochim. Acta 153, 149–168. https://doi.org/10.1016/j.gca.2015.01.007.

Korenaga, J., 2018. Estimating the formation age distribution of continental crust by unmixing zircon ages. Earth Planet. Sci. Lett. 482, 388–395. https://doi.org/10.1016/j.epsl.2017.11.039.

Lackey, J.S., Valley, J.W., Chen, J.H., Stockli, D.F., 2008. Dynamic magma systems, crustal recycling, and alteration in the Central Sierra Nevada batholith: the oxygen isotope record. J. Petrol. 49 (7), 1397–1426. https://doi.org/10.1093/petrology/egn030.

Laurent, O., Martin, H., Moyen, J.F., Doucelance, R., 2014. The diversity and evolution of late-Archean granitoids: evidence for the onset of "modern-style" plate tectonics between 3.0 and 2.5 Ga. Lithos 205, 208–235. https://doi.org/10.1016/J.LITHOS.2014.06.012.

Marschall, H.R., Schumacher, J.C., 2012. Arc magmas sourced from mélange diapirs in subduction zones. Nat. Geosci. 5 (12), 862–867. https://doi.org/10.1038/ngeo1634. Nature Publishing Group.

Miller, J.A., Cartwright, I., Buick, I.S., Barnicoat, A.C., 2001. An O-isotope profile through the HP-LT Corsican ophiolite, France and its implications for fluid flow during subduction. Chem. Geol. 178 (1–4), 43–69. https://doi.org/10.1016/S0009-2541(00)00428-9.

Moyen, J.F., Janoušek, V., Laurent, O., Bachmann, O., Jacob, J.B., Farina, F., Fiannacca, P., Villaros, A., 2021. Crustal melting vs. fractionation of basaltic magmas: part 1, granites and paradigms. Lithos 402–403, 106291. https://doi.org/10.1016/J.LITHOS.2021.106291.

Muehlenbachs, K., 1998. The oxygen isotopic composition of the oceans, sediments and the seafloor. Chem. Geol. 145 (3–4), 263–273. https://doi.org/10.1016/S0009-2541(97)00147-2.

Mulcahy, S.R., Roeske, S.M., McClelland, W.C., Ellis, J.R., Jourdan, F., Renne, P.R., Vervoort, J.D., Vujovich, G.I., 2014. Multiple migmatite events and cooling from granulite facies metamorphism within the Famatina arc margin of northwest Argentina. Tectonics 33 (1), 1–25. https://doi.org/10.1002/2013TC003398.

Müntener, O., Ulmer, P., 2018. Arc crust formation and differentiation constrained by experimental petrology. Am. J. Sci. 318 (1), 64–89. https://doi.org/10.2475/01.2018.04.

Ni, H., Zhang, L., Xiong, X., Mao, Z., Wang, J., 2017. Supercritical fluids at subduction zones: evidence, formation condition, and physicochemical properties. Earth-Sci. Rev. 167, 62–71. https://doi.org/10.1016/J.EARSCIREV.2017.02.006.

Otamendi, J.E., Tibaldi, A.M., Vujovich, G.I., Viñao, G.A., 2008. Metamorphic evolution of migmatites from the deep Famatinian arc crust exposed in Sierras Valle Fértil–La Huerta, San Juan, Argentina. J. South Am. Earth Sci. 25 (3), 313–335. https://doi.org/10.1016/J.JSAMES.2007.09.001.

Otamendi, J.E., Ducea, M.N., Cristofolini, E.A., Tibaldi, A.M., Camilletti, G.C., Bergantz, G.W., 2017. U-Pb ages and Hf isotope compositions of zircons in plutonic rocks from the central Famatinian arc, Argentina. J. South Am. Earth Sci. 76, 412–426. https://doi.org/10.1016/j.jsames.2017.04.005.

Otamendi, J.E., Ducea, M.N., Tibaldi, A.M., Bergantz, G.W., de la Rosa, J.D., Vujovich, G.I., 2009. Generation of tonalitic and dioritic magmas by coupled partial melting of gabbroic and metasedimentary rocks within the deep crust of the Famatinian magmatic arc, Argentina. J. Petrol. 50 (5), 841–873. https://doi.org/10.1093/petrology/egp022.

Otamendi, J.E., Cristofolini, E.A., Morosini, A., Armas, P., Tibaldi, A.M., Camilletti, G.C., 2020. The geodynamic history of the Famatinian arc, Argentina: a record of exposed geology over the type section (latitudes 27°-33° south). J. South Am. Earth Sci. 100, 102558. https://doi.org/10.1016/j.jsames.2020.102558.

Plank, T., Langmuir, C.H., 1998. The chemical composition of subducting sediment and its consequences for the crust and mantle. Chem. Geol. 145 (3–4), 325–394. https://doi.org/10.1016/S0009-2541(97)00150-2.

Puetz, S.J., Spencer, C.J., Ganade, C.E., 2021. Analyses from a validated global UPb detrital zircon database: enhanced methods for filtering discordant UPb zircon analyses and optimizing crystallization age estimates. Earth-Sci. Rev. 220, 103745. https://doi.org/10.1016/J.EARSCIREV.2021.103745.

Ramacciotti, C., Casquet, C., Baldo, E., Galindo, C., Ramacciotti, C., Casquet, C., Baldo, E., Galindo, C., 2015. The Difunta Correa metasedimentary sequence (NW Argentina): relict of a Neoproterozoic platform? - elemental and Sr-Nd isotope evidence. Rev. Mex. Cienc. Geol. 32 (3), 395–414. http://www.scielo.org.mx/scielo.php?script=sci_arttext&pid=S1026-87742015000300395&lng=es&nrm=iso&tlng=.

Ramos, V.A., 2004. Cuyania, an exotic block to Gondwana: review of a historical success and the present problems. Gondwana Res. 7 (4), 1009–1026. https://doi.org/10.1016/S1342-937X(05)71081-9.

Rapela, C.W., Pankhurst, R.J., Casquet, C., Dahlquist, J.A., Mark Fanning, C., Baldo, E.G., Galindo, C., Alasino, P.H., Ramacciotti, C.D., Verdecchia, S.O., Murra, J.A., Basei, M.A.S., 2018. A review of the Famatinian Ordovician magmatism in southern South America: evidence of lithosphere reworking and continental subduction in the early proto-Andean margin of Gondwana. Earth-Sci. Rev. 187, 259–285. https://doi.org/10.1016/j.earscirev.2018.10.006. Elsevier.

Roberts, N.M.W., Slagstad, T., Parrish, R.R., Norry, M.J., Marker, M., Horstwood, M.S.A., 2013. Sedimentary recycling in arc magmas: geochemical and U-Pb-Hf-O constraints on the Mesoproterozoic Suldal Arc, SW Norway. Contrib. Mineral. Petrol. 165 (3), 507–523. https://doi.org/10.1007/s00410-012-0820-y.

Roberts, N.M.W., Spencer, C.J., 2015. The zircon archive of continent formation through time. GSL Spec. Publ. 389 (1), 197–225. https://doi.org/10.1144/SP389.14.

Rudnick, R.L., Gao, S., 2003. Composition of the Continental Crust. Treatise on Geochemistry, vol. 3–9. Elsevier, pp. 1–64.

Salters, V.J.M., Stracke, A., 2004. Composition of the depleted mantle. Geochem. Geophys. Geosyst. 5 (5), 5–07. https://doi.org/10.1029/2003GC000597.

Scholl, D.W., von Huene, R., 2009. Implications of estimated magmatic additions and recycling losses at the subduction zones of accretionary (non-collisional) and collisional (suturing) orogens. GSL Spec. Publ. 318 (1), 105–125. https://doi.org/10.1144/SP318.4.

Spencer, C.J., Cavosie, A.J., Morrell, T.R., Lu, G.M., Liebmann, J., Roberts, N.M.W., 2022. Disparities in oxygen isotopes of detrital and igneous zircon identify erosional bias in crustal rock record. Earth Planet. Sci. Lett. 577, 117248. https://doi.org/10.1016/J.EPSL.2021.117248.

Spencer, C.J., Cavosie, A.J., Raub, T.D., Rollinson, H., Jeon, H., Searle, M.P., Miller, J.A., McDonald, B.J., Evans, N.J., 2017. Evidence for melting mud in Earth's mantle from extreme oxygen isotope signatures in zircon. Geology 45 (11), 975–978. https://doi.org/10.1130/G39402.1.

Stern, R.J., Scholl, D.W., 2010. Yin and Yang of continental crust creation and destruction by plate tectonic processes. Int. Geol. Rev. 52 (1), 1–31. https://doi.org/10.1080/00206810903332322.

Storck, J.C., Wotzlaw, J.F., Karakas, Ö., Brack, P., Gerdes, A., Ulmer, P., 2020. Hafnium isotopic record of mantle-crust interaction in an evolving continental magmatic system. Earth Planet. Sci. Lett. 535, 116100. https://doi.org/10.1016/j.epsl.2020.116100.

Tatsumi, Y., Kogiso, T., 2003. The subduction factory: its role in the evolution of the earth's crust and mantle. GSL Spec. Publ. 219 (1), 55–80. https://doi.org/10.1144/GSL.SP.2003.219.01.03.

Thomas, W.A., Astini, R.A., 2003. Ordovician accretion of the Argentine Precordillera terrane to Gondwana: a review. J. South Am. Earth Sci. 16 (1), 67–79. https://doi.org/10.1016/S0895-9811(03)00019-1.

Tibaldi, A.M., Otamendi, J.E., Cristofolini, E.A., Baliani, I., Walker, B.A., Bergantz, G.W., 2013. Reconstruction of the Early Ordovician Famatinian arc through thermobarometry in lower and middle crustal exposures, Sierra de Valle Fértil, Argentina. Tectonophysics 589, 151–166. https://doi.org/10.1016/j.tecto.2012.12.032.

Trail, D., Bruce Watson, E., Tailby, N.D., 2012. Ce and Eu anomalies in zircon as proxies for the oxidation state of magmas. Geochim. Cosmochim. Acta 97, 70–87. https://doi.org/10.1016/J.GCA.2012.08.032.

Ulmer, P., Kaegi, R., Müntener, O., 2018. Experimentally derived intermediate to silica-rich arc magmas by fractional and equilibrium crystallization at 1 · 0 GPa: an evaluation of phase relationships, compositions, liquid lines of descent and oxygen fugacity. J. Petrol. 59 (1), 11–58. https://doi.org/10.1093/petrology/egy017.

van Staal, C.R., Vujovich, G.I., Currie, K.L., Naipauer, M., 2011. An Alpine-style Ordovician collision complex in the Sierra de Pie de Palo, Argentina: record of

subduction of Cuyania beneath the Famatina arc. J. Struct. Geol. 33 (3), 343–361. https://doi.org/10.1016/j.jsg.2010.10.011.

Vervoort, J.D., Blichert-Toft, J., 1999. Evolution of the depleted mantle: Hf isotope evidence from juvenile rocks through time. Geochim. Cosmochim. Acta 63 (3–4), 533–556. https://doi.org/10.1016/S0016-7037(98)00274-9.

Vervoort, J.D., Plank, T., Prytulak, J., 2011. The Hf-Nd isotopic composition of marine sediments. Geochim. Cosmochim. Acta 75 (20), 5903–5926. https://doi.org/10.1016/j.gca.2011.07.046.

Walker, B.A., Bergantz, G.W., Otamendi, J.E., Ducea, M.N., Cristofolini, E.A., 2015. A MASH zone revealed: the mafic complex of the Sierra Valle Fértil. J. Petrol. 56 (9), 1863–1896. https://doi.org/10.1093/petrology/egv057.

Wiedenbeck, M., Hanchar, J.M., Peck, W.H., Sylvester, P., Valley, J., Whitehouse, M., Kronz, A., Morishita, Y., Nasdala, L., Fiebig, J., Franchi, I., Girard, J.P., Greenwood, R.C., Hinton, R., Kita, N., Mason, P.R.D., Norman, M., Ogasawara, M., Piccoli, P.M., et al., 2004. Further characterisation of the 91500 zircon crystal. Geostand. Geoanal. Res. 28 (1), 9–39. https://doi.org/10.1111/j.1751-908X.2004.tb01041.x.

Wotzlaw, J.F., Buret, Y., Large, S.J.E., Szymanowski, D., Von Quadt, A., 2017. ID-TIMS U–Pb geochronology at the 0.1‰ level using 10^{13} Ω resistors and simultaneous U and $^{18}O/^{16}O$ isotope ratio determination for accurate UO 2 interference correction. J. Anal. At. Spectrom. 32 (3), 579–586. https://doi.org/10.1039/C6JA00278A.